JOURNAL OF NEUROTRAUMA 32:1001–1010 (July 1, 2015)

DOI: 10.1089/neu.2014.3737

Manganese-Enhanced Magnetic Resonance Imaging of Traumatic Brain Injury

Lora Talley Watts,[1–3] Qiang Shen,[1,4] Shengwen Deng,[1] Jonathan Chemello,[1] and Timothy Q. Duong[1,4,5]

Abstract

Calcium dysfunction is involved in secondary traumatic brain injury (TBI). Manganese-enhanced MRI (MEMRI), in which the manganese ion acts as a calcium analog and a MRI contrast agent, was used to study rats subjected to a controlled cortical impact. Comparisons were made with conventional T2 MRI, sensorimotor behavior, and immunohistology. The major findings were: (1) Low-dose manganese (29 mg/kg) yielded excellent contrast with no negative effects on behavior scores relative to vehicle; (2) T1-weighted MEMRI was hyperintense in the impact area at 1–3 h, hypointense on day 2, and markedly hypointense with a hyperintense area surrounding the core on days 7 and/or 14, in contrast to the vehicle group, which did not show a biphasic profile; (3) in the hyperacute phase, the area of hyperintense T1-weighted MEMRI was larger than that of T2 MRI; (4) glial fibrillary acidic protein staining revealed that the MEMRI signal void in the impact core and the hyperintense area surrounding the core on day 7 and/or 14 corresponded to tissue cavitation and reactive gliosis, respectively; (5) T2 MRI showed little contrast in the impact core at 2 h, hyperintense on day 2 (indicative of vasogenic edema), hyperintense in some animals but pseudonormalized in others on day 7 and/or 14; (6) behavioral deficit peaked on day 2. We concluded that MEMRI detected early excitotoxic injury in the hyperacute phase, preceding vasogenic edema. In the subacute phase, MEMRI detected contrast consistent with tissue cavitation and reactive gliosis. MEMRI offers novel contrasts of biological processes that complement conventional MRI in TBI.

Key words: calcium activity; controlled cortical impact; cortical spreading depolarization; gliosis; MEMRI; TBI

Introduction

Traumatic brain injury (TBI) affects 3.5 million Americans with an annual cost exceeding $60 billion.[1] The primary insult is followed by secondary injuries such as excitotoxic injury, vasogenic edema, inflammation, and gliosis (among others), spreading over the course of hours to months.[2,3] Calcium plays an important role in normal cellular function. Calcium activity is perturbed in many of the secondary injury cascades in TBI. Excitotoxic injury, for example, could activate voltage-gated calcium channels and increase influx of calcium into cells,[4] which could cause further cellular damage and cell death.[5] Reactive gliosis, which forms a scar around the injury site, acts as a protective measure and is known to involve calcium signaling and activity.[6,7] Thus, the ability to longitudinally image calcium activity could offer novel insight into the pathogenesis of TBI.

Manganese-enhanced MRI (MEMRI), in which the manganese ion (Mn^{2+}) is used as a calcium analog and an MRI contrast agent, is sensitive to a number of biological processes.[8] MEMRI has been widely used to investigate structure, function, and functional connectivity in animal models. Mn^{2+} enters cells through active voltage-gated calcium channels, but unlike calcium, Mn^{2+} is trapped inside cells with a long half-life (on the order of days). This property allows functional encoding to be done at one time point usually in awake and behaving conditions and *in vivo* imaging at another.

MEMRI is typically acquired using conventional T1 imaging techniques that yield higher spatial resolution and signal-to-noise ratio, compared with echo-planar imaging techniques commonly used in blood-oxygenation-level-dependent functional MRI studies. MEMRI has been used to map brain function with intravenous Mn^{2+} administration[9,10] where blood–brain barrier (BBB) disruption is needed to deliver sufficient Mn^{2+} to the brain. MEMRI has also been used to provide anatomical contrast after intravenous or intraperitoneal Mn^{2+} administration a few hours to a day before imaging without breaking the BBB, because Mn^{2+} can slowly cross the BBB and different cell types in the brain have different basal levels of calcium activity.[8]

Mn^{2+} is also packaged and transported across synapses like calcium and thus can be used for fiber tracking when Mn^{2+} is

[1]Research Imaging Institute, [2]Departments of Cellular and Structure Biology, [3]Neurology, [4]Ophthalmology, University of Texas Health Science Center, San Antonio, Texas.
[5]South Texas Veterans Health Care System, San Antonio, Texas.

delivered via intranasal[11] or intracerebral[12] administration routes. A disadvantage of MEMRI is that it cannot be used to dynamically image functional changes in real time, and a disrupted BBB is usually needed for imaging stimulus-evoked responses. MEMRI has also been applied to study animal models of neurological diseases, including stroke,[13] Alzheimer disease,[14] lupus,[15] and fluid percussion injury.[16] MEMRI has also been used to study inflammatory gliosis.[6]

The purpose of this study was to explore the use of MEMRI to investigate an open-skull controlled cortical impact model of moderate TBI in rats. MEMRI was compared with conventional T2 MRI, immunohistology (glial fibrillary acidic protein, GFAP), and sensorimotor behavioral measurements. We hypothesized that MEMRI provides novel and useful contrasts to TBI pathophysiology, offering complementary information to conventional anatomical T2 MRI in TBI.

Methods

Animal preparation

All animal procedures were approved by the Institutional Animal Care and Use Committee of the University of Texas Health Science Center, San Antonio. Male Sprague Dawley rats (250–350 g) were anesthetized initially with 5% isoflurane mixed with room air, maintained with 2% isoflurane during surgery, and 1.5% during imaging procedures.

The experimental design is shown in Figure 1. Three groups were studied: (1) High-dose Mn^{2+} (88 mg $MnCl_2$*$4H_2O$ per kg, n = 4), in which a 120 mM $MnCl_2$*$4H_2O$ solution was administered at 1.8 mL/h over 30 min via tail vein starting 1 h before TBI (day 0), and again on days 1, 6, and 13 after TBI. (2) Low-dose Mn^{2+} (29 mg $MnCl_2$*$4H_2O$ per kg, n = 6), in which a 40 mM $MnCl_2$*$4H_2O$ solution was administered at 1.8 mL/h over 30 min at the same time points described in group 1. (3) Vehicle (n = 6), in which saline was infused over 30 min and administered at the same time points as in group 1. During the high dose Mn^{2+} infusion, heart rate and mean arterial blood pressure were mildly and transiently reduced, whereas during low dose Mn^{2+} infusion, the values were within normal ranges. Body temperature (36.5–37.5°C), heart rate (350–450 bpm), and mean arterial blood pressure (120–170 mmHg) during MRI were all within normal ranges.

After Mn^{2+} or vehicle infusion on the day of the TBI (day 0), the animal was secured in a stereotaxic frame and a Ø5 mm craniotomy was created over the left somatosensory cortex (S1: +0.25 mm anterior and 3.5 mm lateral to bregma), exposing the dura matter. The intact dura matter was impacted using a pneumatic controlled cortical impactor (Precision Systems and Instrumentation, LLC, Fairfax Station, VA) fitted with a Ø3 mm tip. The impact was induced using 5.0 m/sec, 250 μs dwell time, and a 1 mm depth to mimic a moderate focal TBI.[17] After the impact, the cranial opening was sealed with bone wax, the scalp sutured closed, and antibiotic ointment applied along the suture line. The analgesic buprenorphine (0.05 mg/kg) was given subcutaneously every 12 h as needed for pain for 3 days.

MRI was performed at 1–3 h, and 1, 2, 7, and 14 days post-TBI for groups 2 and 2. MRI of group 3 (vehicle) was performed at 2 h, 2, 7, and 14 days post-TBI with an additional MRI performed on day 15. Note that Mn^{2+} or vehicle was injected via tail vein 30 min before TBI (day 0), and 24 h before MRI on days 1, 6, and 13 for groups 1 and 2 and on days 1, 6, 13, and 14 for group 3 (Fig. 1).

MRI

MRI studies were performed on a 7 Tesla Pharmascan (Bruker, Billerica, MA). The anesthetized animals were secured in an MRI-compatible stereotaxic holder with ear and tooth bars. A transceiver surface coil of 2 cm in diameter was placed over the intact skull.[18]

RARE (rapid acquisition with relaxation enhancement). T2-weighted images were acquired using a fast spin-echo sequence with repetition time (TR) = 3 sec (90-degree flip angle), effective echo time (TE) = 18, 54, 90, and 126 msec, 4 echo train length, seven 1.0-mm thick coronal images, field of view (FOV) = 2.56 × 2.56 cm, matrix 96 × 96 and reconstructed to 128 × 128, and eight transients for signal averaging. There were no gaps between slices. T2 maps were calculated.

IR-RARE (Inversion Recovery RARE. T1-weighted MEMRI images were acquired using an IR-RARE sequence with TR = 3 sec, inversion delay (TI) = 1 sec, seven 1.0-mm thick coronal images, field of view = 2.56 × 2.56 cm, matrix 128 × 128, and four transients for signal averaging. There were no gaps between slices.

Images were co-registered across time points using QuickVol and MRIAnalysisPak software.[19] The lesion volumes were determined as pixels that had T2 values higher than the mean plus two standard deviations of the value in the homologous contralesional hemisphere.[20] T1-weighted signal intensities were analyzed for two (core and surround) regions of interest (ROIs) in the low-dose Mn^{2+} group. The intensities were normalized with respect to the signal intensity of the homologous ROI in the contralateral hemisphere in the same animal. The T1-weighted signal intensity profiles were correlated with behavioral scores. Comparison was also made with the vehicle group.

Behavioral assessment

Sensorimotor function was assessed using the asymmetry forelimb placement (cylinder) test and foot-fault test. Baseline behavioral assessments[21] were made before the induction of TBI and Mn^{2+} infusion. Behavioral assessments were also performed

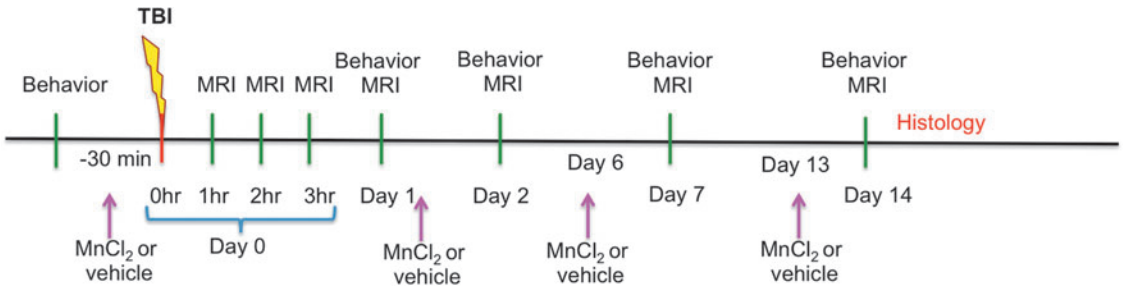

FIG. 1. Experimental design shows behavioral, magnetic resonance imaging (MRI), and histological measurements as well as the time points of manganese chloride ($MnCl_2$) or vehicle administration. TBI, traumatic brain injury. Color image is available online at www.liebertpub.com/neu

before MRI acquisition on days 1, 2, 7, and 14 post-TBI. Behavioral tests were not performed after TBI induction on day 0 because of incomplete recovery from anesthesia.

The forelimb asymmetry placement test was performed by placing a rat into a transparent cylinder (20 cm diameter, 30 cm height) for 5 min or until 30 placements were made.[17] A mirror positioned under the cylinder enabled a video recorder to see directly into the cylinder. The behavior was scored by counting the number of left or right individual forelimb placements and the number of simultaneous right and left (both) forelimb placements onto the cylinder wall during rearing. The forelimb asymmetry index was calculated as (the number of forelimb placements for each individual limb) + ½ (the number of both placements) divided by the total number of placements.

The foot fault test was performed[17] to assess limb misplacement during locomotion. The rat was placed on an elevated grid floor (e.g., size 18 in × 11 in with grid openings of ~1.56 in^2 and 1 in^2) for 5 min or until 50 steps were taken with one (right) forelimb. The rat was allowed to move freely on the grid, and the total number of steps and the number of foot faults through the grid openings were counted. The percentage of foot faults for each limb was calculated as the number of right or left forelimb foot faults divided by the total number of steps taken with the right forelimb.

Histology

For histological correlation with MRI immunohistology for GFAP was assessed immediately after MRI experiments on day 14 post-TBI. The 14-day end-point was chosen based on a subset of studies in which no apparent differences in lesion volumes were observed between 14 and 28 days post-TBI.

Briefly, selected rats were perfused 14 days post-TBI with ice-cold 5% sucrose in heparinized phosphate buffered saline (PBS), followed by ice-cold 4% buffered paraformaldehyde. Brains were removed and post-fixed for 2–5 h at 4°C and subsequently cryopreserved in 30% sucrose for 2 days. 30-μm thick coronal sections were mounted on gelatin-coated slides and stored at −20°C. Sections were processed using standard immunofluorescent staining against GFAP.

Briefly, sections were washed with PBS followed by permeabilization using 0.2% Triton X-100 (2 μl Triton X-100:1 mL PBS). The sections were blocked with 10% goat serum followed by incubation with a primary antibody directed against GFAP diluted in goat serum (1:1000 GenScript Rabbit Anti-GFAP pAb Cat# A01309) overnight at 4°C. The slides were then washed with PBS and incubated with secondary antibody (1:80 Sigma Aldrich Anti-Rabbit IgG-FITC Antibody Cat# MFCD00162786) for 1 h at 37°C. Slides were washed and mounted with Vectashield containing DAPI (Vector Laboratories). Images were acquired on a Nikon C1si microscope using 10X, 20X, and 60X objectives.

Statistical analysis

Mann-Whitney *U* tests were used to compare differences in asymmetrical limb use and the percentage of foot faults between vehicle-and Mn^{2+}-treated animals. Values are presented as mean ± standard error of the mean. Statistical significance was set at $p < 0.05$.

Results

High Mn dose (group 1)

Representative T2 maps and IR T1-weighted images 2 h post-TBI after a high Mn^{2+} dose are shown in Figure 2A. TBI alone resulted in T2 abnormality (increases) peaking on day 2, consistent with those reported previously.[17] Heterogeneous T1-weighted signal enhancement was evident in the cerebrospinal fluid (CSF) of the lateral ventricles (arrows) unrelated to TBI, as expected. TBI induced little or no T2 contrast in the ipsilesional cortex under the impact area at 2 h compared with the contralesional cortex. By comparison, T1-weighted MRI showed an apparent and heterogeneously hyperintense lesion that extended beyond the cortex immediately below the impact. MRI enhancement appeared saturated in the impact area, likely because of the high Mn^{2+} concentration present.

TBI resulted in behavioral deficits peaking on day 2, consistent with those reported previously.[17] TBI resulted in worsening of asymmetry and foot fault scores on day 1 and 2 (Fig. 2B). Before TBI, the mean forelimb asymmetry scores were not significantly different between the vehicle and high Mn^{2+} dose group (52 ± 2% vs. 51 ± 2%, $p > 0.05$ respectively). After TBI, the forelimb asymmetry scores were statistically different between the high-dose and saline group on days 2 and 7 ($p = 0.044$ and 0.048 respectively).

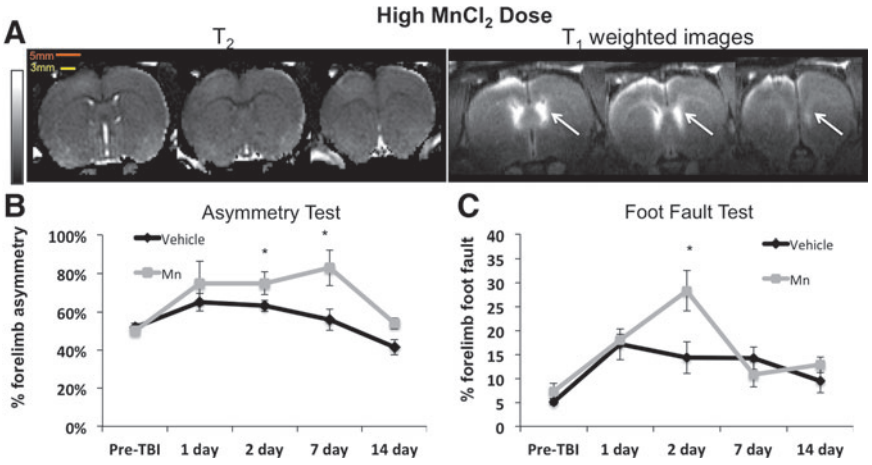

FIG. 2. (**A**) High manganese ion (Mn^{2+}) dose (group 1) T2 maps and T1-weighted images 2 h after TBI and 3 h after Mn^{2+} administration from the same animal. Hyperintensity was observed in the lateral ventricles (arrows) and in the apparent lesion. The scale bars indicate the size of the bird hole (5 mm) and the impactor tip (3 mm). The scale bar indicates T2 of 0–100 msec. (**B**) Group-averaged forelimb asymmetry and (**C**) foot fault scores at different time points. N = 4 for high dose (group 1), n = 6 for vehicle (group 3); error bars are standard error of the mean, and * indicates $p < 0.05$. $MnCl_2$, manganese chloride; TBI, traumatic brain injury. Color image is available online at www.liebertpub.com/neu

Similarly, before TBI, the foot fault scores of the high-dose group were not significantly different compared with the vehicle group (7.33 ± 0.44% and 5.13 ± 0.58%) (Fig. 2C). After TBI, the foot fault scores were statistically different between the high-dose and saline group on day 2 ($p = 0.019$). These behavioral data indicated that the high Mn^{2+} dose had additional negative side effects on behavior.

Low Mn dose (group 2)

To minimize potential Mn^{2+} toxicity and signal saturation of MRI signal enhancement, the Mn^{2+} dose was lowered (Fig. 3A). Low-dose Mn^{2+} yielded adequate contrast in the cortex below the impact, and the T1 enhancement also appeared less saturated. Compared with the contralesional cortex, TBI again induced little or no apparent T2 abnormality (increases) in the ipsilesional cortex under the impacted area at 2 h. By comparison, T1-weighted images showed an apparent lesion (heterogeneous hyperintensity) that extended beyond the cortex below the impact.

For animals both before and after TBI, the forelimb asymmetry and foot fault scores were not significantly different between the low-dose Mn^{2+} and the vehicle group (Fig. 3B, C). The overall physical activity was not different between the low dose and vehicle groups at all time points (data not shown). These behavioral data indicated that low Mn^{2+} dosing had no additional negative effects on behavior compared with the vehicle group. Thus, subsequent studies used only the low Mn^{2+} dose.

Longitudinal MEMRI (group 2)

Representative time-series T2 maps and T1-weighted images at 2 h and again on 2, 7, and 14 days post-TBI from two animals are shown in Figure 4. At 2 h, little or no apparent T2 changes were visible in the tissue immediately below the impact, whereas hyper- and hypointensities were detected in T1-weighted images in and around the impact area.

On day 2, the T2 map indicated hyperintense areas within the impact area, whereas MEMRI reversed from hyperintensity on day 0 to hypointensity on day 2 with heterogeneous contrasts. The T2 maps and T1-weighted images showed different contrasts. Lesions defined by T2 maps and T1-weighted images appeared qualitatively similar in size.

On day 7, T2 contrast reversed and became mostly hypointense, likely because of T2 reduction by Mn^{2+}, with some hyperintensity on the cortical surface. By comparison, T1-weighted MRI showed a large signal void immediately underneath the impact area. T1-weighted images also showed a crescent-shaped hyperintensity on day 7 in some animals (Fig. 4B) and/or day 14 in others (Fig. 4A).

On day 14, the T2 maps remained hyperintense (albeit less) in some animals (Fig. 4A) and pseudonormalized in others (Fig. 4B). By comparison, T1-weighted images showed a signal void immediately below the impact area and a crescent-shaped hyperintensity surrounding the signal void on day 7 and/or day 14. In general, hypointense cavitation and hyperintense regions surrounding the cavitation were observed on day 7 and/or 14.

Vehicle control (group 3)

To evaluate the possible T1 changes from TBI independent of Mn^{2+} contrast enhancement, animals were injected with saline (vehicle) and imaged. Representative T2 maps and T1-weighted images at 2 h and again on 2, 7, and 14 days post-TBI with vehicle administration are shown in Figure 5. In contrast to group 2, there was no significant T1-weighted enhancement in the cortex below the impact area and no signal void in impact core on T1-weighted MRI. Instead, a relatively constant hypointensity was observed in the core at all the time points studied. No significant changes in the surrounding area were detected at all the time points studied. In addition, T2 pseudonormalized earlier in group 3 than in group 2.

The lesion volumes of groups 1, 2, and 3 were not statistically different from each other (15.2 ± 3.4, 13.87 ± 2.9 and 17.3 ± 4.4 mm^3, respectively) on day 2.

Quantitative analysis

In the low-dose Mn^{2+} group (group 2), the normalized signal intensities for two (core and surround) ROIs were tabulated (Fig. 6A). IR T_1-weighted signals were normalized to the homologous

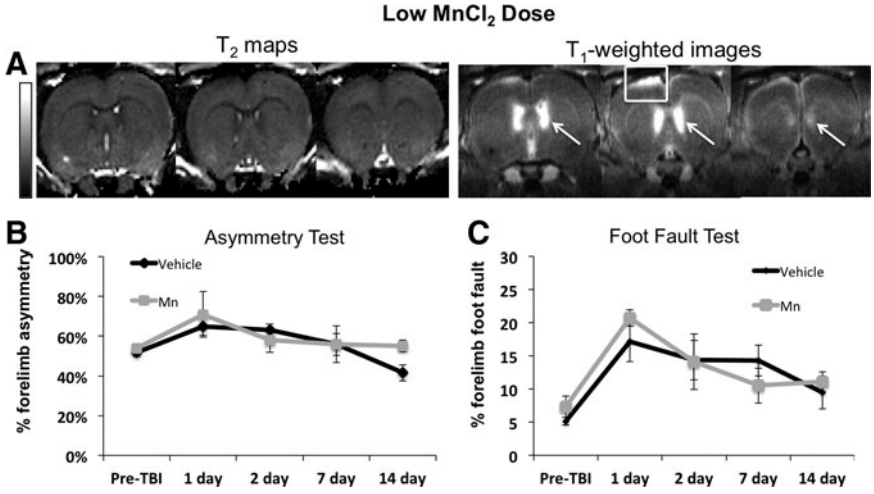

FIG. 3. (**A**) Low manganese ion (Mn^{2+}) dose (group 2) T2 maps and T1-weighted images 2 h after traumatic brain injury (TBI) and 3 h after Mn^{2+} administration from the same animal. T2 maps showed no changes while T1-weighted images had sufficient signal enhancement similar to the high dose in the lateral ventricles (white arrows) and the apparent lesion (white box). (**B**) Group-averaged forelimb asymmetry and (**C**) foot fault scores at different time points. Error bars are standard error of the mean. N = 6 for the low dose (group 2). N = 6 for the vehicle (group 3). The scale bar indicates T2 of 0–100 msec. $MnCl_2$, manganese chloride.

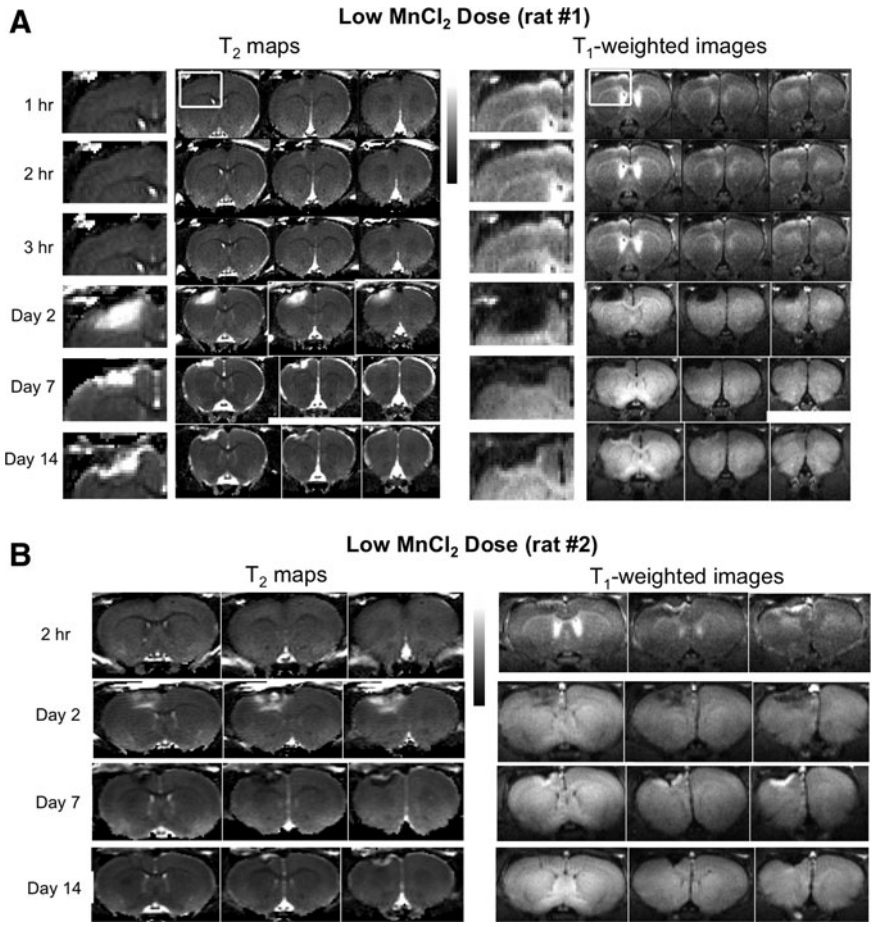

FIG. 4. T2 maps and T1-weighted image time courses after manganese ion (Mn^{2+}) administration from two animals of the low Mn^{2+} dose (group 2). In (**A**), the crescent-shaped hyperintensity was most apparent on day 14 and in (**B**) on day 7. The scale bar indicates T_2 of 0–100 msec. $MnCl_2$, manganese chloride.

regions in the contralesional hemisphere. The central region of the impact was hyperintense (>unity) 1–3 h post-TBI, markedly hypointense (<unity) on day 1, and less hypointense on day 7 and 14, showing the biphasic temporal profile. In contrast, the area surrounding the central region only showed hyperintensity on 7 and 14 days post-TBI.

In the vehicle-treated animals (group 3) by comparison, the central region of the impact showed relatively constant hypointensity throughout the time points studied post-TBI, without the biphasic profile. The surrounding ROI also showed relatively constant hypointensity (absence of hyperintensity in contrast to the Mn^{2+} group) across all time points studied (Fig. 6B).

The normalized T1-weighted intensity profiles from the pre-TBI, day 2, 7, and 14 were correlated with behavioral scores. Although T1-weighted MRI was not performed pre-TBI, its normalized intensity was not expected to differ from unity. The normalized intensity was thus assumed to be 1 in the correlation with behavioral scores. In the low-dose Mn^{2+} group, the correlation coefficient

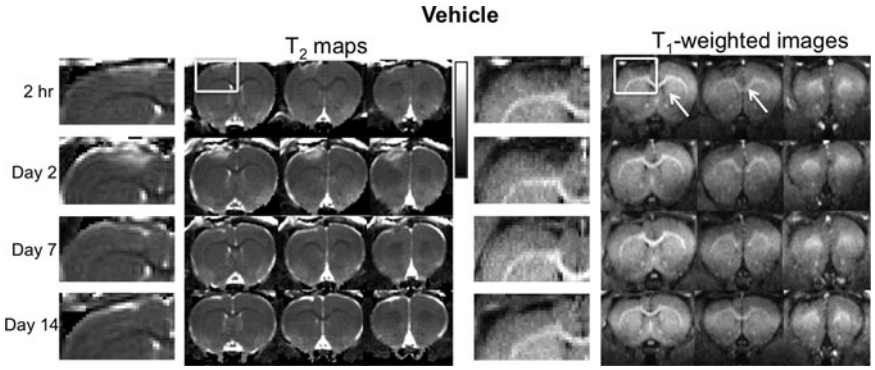

FIG. 5. T2 maps and T1-weighted image time courses after manganese ion (Mn^{2+}) administration from the vehicle group (group 3, no Mn administration). The scale bar indicates T2 of 0–100 msec.

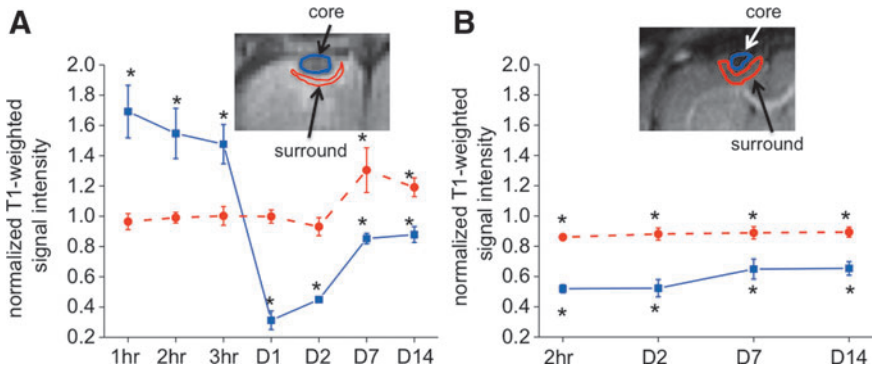

FIG. 6. Normalized signal intensities for two (core and surround) regions of interest of the **(A)** low-dose Mn^{2+} group (group 2) and **(B)** vehicle group (group 3) at different time points. Inversion-recovery T1-weighted signals were normalized to the homologous regions in the contralesional hemisphere. The insets show the typical regions of interest. N = 6 each group, ± standard error of the mean. $*p < 0.05$ from unity. Color image is available online at www.liebertpub.com/neu

between the intensity profile and forelimb asymmetry score was R = −0.89, $p = 0.04$, and between the intensity profile with foot fault score was R = −0.94, $p = 0.02$. In the vehicle group, no significant correlations were observed.

GFAP immunostaining

To further investigate the strong crescent-shaped T1-weighted signal enhancement surrounding the impact region on days 7 and/or 14 and the signal void on day 14, immunohistochemistry was performed on animals in group 2 after MRI on day 14 (Fig. 7). Immediately below the impact area, a pronounced lesion devoid of GFAP staining was observed, suggesting tissue cavitation. At the border surrounding the void, there was enhanced GFAP staining. The expanded views showed astrocytic processes interdigitated along the lesion border, suggesting the formation of a ''wall'' or scar. These findings indicated that the crescent-shaped T1-weighted signal enhancement surrounding the impact region was because of gliosis.

Discussion

This study demonstrated a novel application of MEMRI in the study of experimental TBI. The major findings were: (1) Low-dose manganese (29 mg/kg) yielded excellent contrast with no negative effects on behavior scores relative to vehicle; (2) T1-weighted MEMRI was hyperintense in the impact area at 1–3 h, hypointense on day 2, and markedly hypointense with a hyperintense area surrounding the core on days 7 and/or 14, in contrast to the vehicle group that did not show the biphasic profile; (3). In the hyperacute phase, the area of hyperintense T1-weighted MEMRI was larger than that of T2 MRI. (4) GFAP staining revealed that the MEMRI signal void in the impact core and the hyperintense surrounding on day 7 and/or 14 corresponded to tissue cavitation and reactive gliosis, respectively. (5) T2 MRI showed little contrast in the impact core at 2 h, hyperintense on day 2 (indicative of vasogenic edema), hyperintense in some animals but pseudonormalized in others on day 7 and/or 14. (6) Behavioral deficit peaked on day 2. (7) Significant correlation was found between IR T1-weighted MEMRI intensity profiles and behavioral scores. MEMRI offers novel contrast that complements conventional MRI in the study of TBI.

Mn^{2+} dosing

It is prudent to minimize the dose of Mn^{2+} needed to reduce cytotoxic injury while achieving adequate contrast. We found that the high Mn^{2+} dose (88 mg/kg) yielded excellent but saturating contrast, and negative side effects on behavioral scores compared with the vehicle group. We also explored a dose of 44 mg/kg and found that it also had negative side effects on behavior (data not shown). The Mn^{2+} dose of 29 mg/kg, however, yielded excellent contrast without additional negative side effects on behavior. We did not investigate the potential toxicity effect of Mn^{2+} by histology because previous studies have addressed this issue and found no significant ill effects.[8] In addition, the low-dose Mn^{2+} is at the lower end of what is commonly used. Further lowering of the Mn^{2+} dose may be possible with alternative pulse sequences.

MEMRI on the day of TBI

The rationale of starting Mn^{2+} infusion (over 30 min) 1 h before TBI was to allow Mn^{2+} to adequately distribute in the blood and tissue such that changes immediately after injury could be detected.[9,10,23] Alternatively, Mn^{2+} infusion could be performed after injury but changes immediately after the impact might be missed. In our study, MRI was performed 2 h after Mn^{2+} injection (1 h after TBI), where the majority of Mn^{2+} has left the circulation and moved into different tissues because of its ability to enter active voltage-gated channels. There was indication of BBB leakage in this open skull TBI model enabling Mn^{2+} to cross the BBB.[22]

One important finding is that MEMRI detected earlier and more sensitive changes than T2 MRI in the hyperacute phase, preceding vasogenic edema in the hyperacute phase. The differential MEMRI contrast in the impact area was time dependent. T1-weighted contrast in the deep neocortex was observed. The source of this signal contrast was likely a result of injury-induced energy failure, which caused adenosine triphosphate (ATP) exhaustion, damaging the sodium-potassium ATPase ion pumps, resulting in anoxic depolarization and calcium influx, and thus Mn^{2+} influx, into cells. This resulted in T1-weighted signal enhancement in MEMRI. This observation also suggests that MEMRI detected early indications of excitotoxic injury in the hyperacute phase. Given that the intact BBB is impermeable to Mn^{2+}, there was likely significant TBI-induced BBB disruption.[24]

Moreover, MEMRI enhancement was most intense along the superficial cortex of the impact area. Such enhancement on either side of the impact area at 1–3 h suggests the presence of cortical spreading depolarization, although this was not independently confirmed by electrophysiology in our study. The pattern of MEMRI enhancement is consistent with a previous report of MEMRI study of spreading depolarization induced by topical potassium-chloride

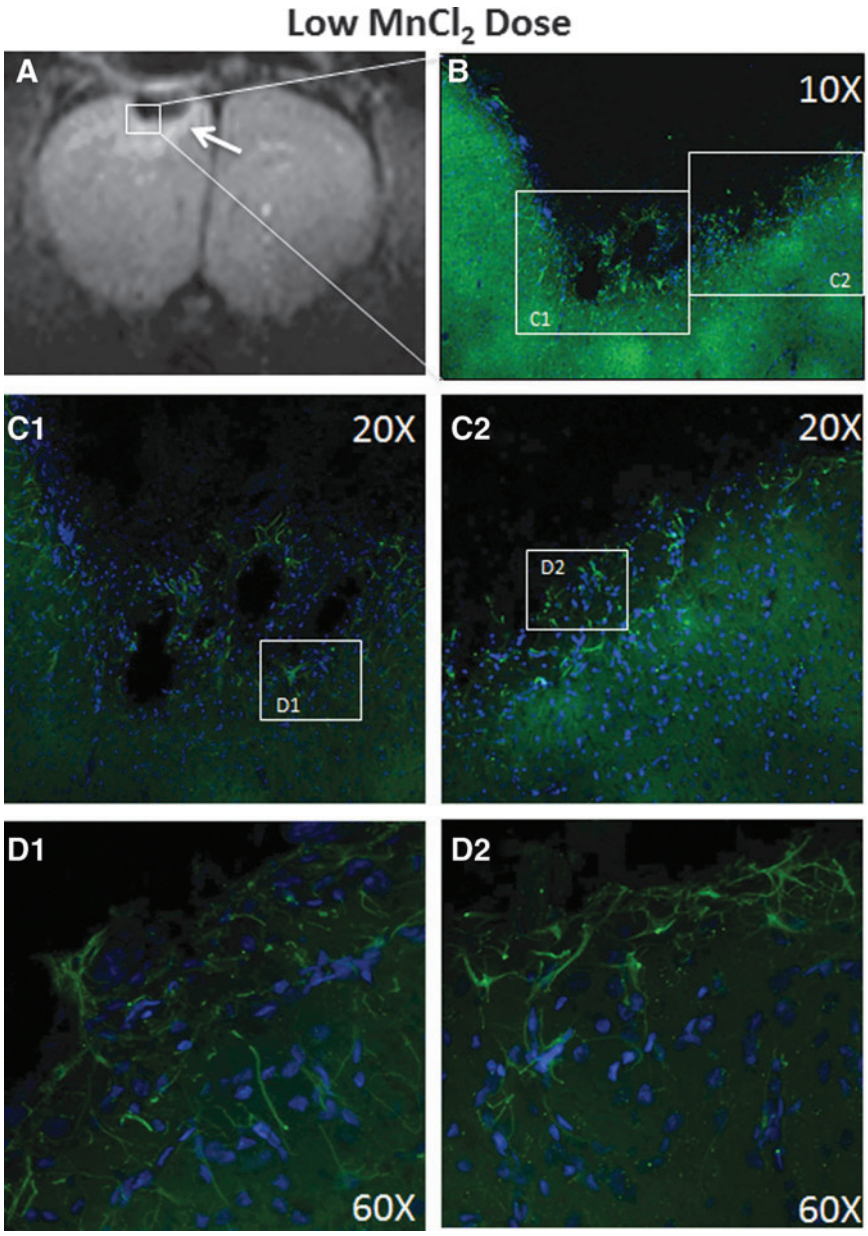

FIG. 7. (**A**) Hyperintense manganese-enhanced contrast observed in T1-weighted images arranged in a crescent shape and surrounding the lesion core on day14 from the low Mn^{2+} dose (group 2). (**B**) Glial fibrillary acidic protein (green) and DAPI (blue) stained glial cells and nuclei, respectively, under a 10X objective collected on a confocal microscope were taken in a portion of the lesion. (**C**) 20X confocal images show a dense accumulation of glial cells along the border surrounding the cortex below the impact. (**D**) 60X confocal images show glial cells close together along the lesion border in a wall-like manner, suggesting gliosis. Astrocytic processes seem to interdigitate at the lesion border. $MnCl_2$, manganese chloride. Color image is available online at www.liebertpub.com/neu

application.[25] While it is clear that MEMRI enhancement was in the tissue (not intravascular blood signal), it is possible that these signal changes along the superficial cortex could be caused by bleeding on the brain surface or simply influx of Mn^{2+} into injured cells but not by spreading depolarization.

MEMRI on days 2–14

The rationale for injecting Mn^{2+} 24 h before subsequent MRI experiments on day 2, 7, and 14 was to investigate the accumulated neural and glial activity over the course of several hours in a manner similar to a previous study.[8] The differential MEMRI contrast compared with the neighboring and contralesional tissue was likely the result of different accumulated calcium activity of neural and glial cells. The cortex below the impact showed markedly reduced T1-weighted signal on days 7 and/or 14, consistent with reduced neuronal activity from injured or dead cells. This interpretation is consistent with tissue cavitation detected by histology.

In addition, there was a crescent-shaped hyperintensity surrounding the signal void on day 7 and/or 14. This was likely the result of increased Mn^{2+} accumulation in glial cells or increased cell migration toward the injury site. This notion was verified to be reactive gliosis by histology (see below), which formed a barrier preventing Mn^{2+} from reaching the injured or dead tissue, thereby

creating the signal void evidenced by the lack of Mn^{2+} enhancement seen in the impact area. The signal void and crescent-shaped hyperintensity typically peaked on day 7 or 14, likely dependent on variations in the extent of injury between animals. Figures 4A and 4B are shown to reflect representative heterogeneous MEMRI contrasts in both space and time. The results were found to be similar in the high Mn^{2+} dose data set (data not shown), further supporting the notion of a hypointense cavity and crescent-shaped enhanced region surrounding the cavitation.

There are alternative interpretations of MEMRI signal changes in TBI, although these are unlikely. It is possible that inversion nulling would occur without Mn^{2+} if the damaged tissue was filled with CSF at day 7 and 14. This is not the case for the following reasons: (1) There was no evidence, based on T2, that the injured tissue immediately below the impact was completely filled with CSF at these time points. (2) The CSF in and around the lateral ventricles across multiple slices with Mn^{2+} was not hypointense; in fact it was mostly hyperintense on T1-weighted MRI (similar to the neighboring tissue) because of Mn^{2+} presence. (3) The vehicle group did show similar T1-weighted hypointensity in the core, consistent with Mn^{2+} group in quantitative normalized T1-weighted signal intensities (Fig. 6). These findings also suggest that there were T1 and T2 increases in the core. We thus concluded that the hypointensity of the injured tissue immediately below the impact was because of the absence of Mn^{2+} infiltration as the result of scar/gliosis.

It is also possible that the dense glial scar per se could have minor T1-weighted hyperintensity, giving rise to the crescent-shaped hyperintensity. The vehicle experiments did not show such T1-weighted hyperintensity, however. We thus concluded the crescent-shaped hyperintensity is associated with Mn^{2+}.

Control experiments

It is possible that TBI could account for the observed T1 changes irrespective of whether Mn^{2+} was injected. To investigate this possibility, control experiments in which animals were injected with saline vehicle were performed. No substantial T1-weighted signal enhancement because of TBI was observed at any time point studied (especially on day 0). Instead, there was hypointensity in the cortex below the impact and it was relatively time invariant. There was also no hyperintensity surrounding the impacted area observed on T1-weighted MRI, in contrast to group 2. These findings support the notion that there was T1 increase in the core in both vehicle and Mn^{2+} groups (Fig. 6), consistent with vasogenic edema. These data support the conclusion that the hypointensity of the injured tissue immediately below the impact was because of the absence of Mn^{2+} infiltration as the result of scar/gliosis, and the hyperintensity in the tissue surrounding the core was from increased calcium activity from reactive gliosis.

In addition, we also found T2 pseudonormalized earlier than those in group 2. There are two possible explanations: Mn^{2+} caused a more severe injury than vehicle, or Mn^{2+} caused T2 shortening in the lesion. The former explanation was less likely because the lesion volumes on day 2 and behavioral scores across all time points were not statistically different between groups 2 and 3. Note that lesion volumes were obtained only on day 2 because they were well defined compared with other time points studied.[17] The latter explanation is likely because Mn^{2+} is known to shorten T2, counteracting the edema T2 increases.

Comparison with a previous MEMRI TBI study

A previous study reported the use of MEMRI after fluid percussion injury.[16] Mn^{2+} was administered via intraperitoneal injection 24 h before each MRI session. No significant changes in MEMRI 24 h after TBI were observed, and it was concluded that MEMRI at 24 h was not predictive of long-term outcome. Differential MEMRI was observed only in the dentate gyrus at 1 month. These findings differed from ours in that we detected changes at 1–3 h, as well as changes on days 1 and 2 after TBI using the controlled cortical impact model.

This discrepancy could be because of differences in the TBI models, the delivery route for Mn^{2+}, and/or the MRI parameters used. The fluid percussion model caused a comparatively more severe injury, where even the sham-operated animals showed dramatic damage on both T2 MRI and T1-weighted MEMRI. This extensive damage could mask the Mn^{2+}-induced contrast. Intraperitoneal and intravenous Mn^{2+} administration yielded different vascular Mn^{2+} profiles, which could account for their finding of no significant changes in MEMRI 24 h after TBI. In addition, their T1-weighted MRI used a short TR gradient-echo acquisition, whereas our study used IR T1-weighted MRI optimized to detect T1 contrast for our Mn^{2+} dosing.

GFAP staining

To probe the MEMRI hyperintensity seen surrounding the area immediately below the impact, we stained for GFAP, an indicator of reactive gliosis after TBI.[17] Our data support the hypothesis that glial scarring contributed to the strong T1-weighted signal enhancement surrounding the impact core. At the boundary surrounding the signal void, glial cells accumulated and astrocytic processes interdigitated at the lesion border suggesting the formation of a ''wall'' or scar (gliosis) that prevented Mn^{2+} delivery to the impact core. The astrocytes surrounding the lesion likely accumulated more Mn^{2+} because of their hyperactivity and/or increased cell density from cell migration toward the injured site as a result of gliosis or inflammatory response.

The activation of astrocytes could have beneficial or harmful effects depending on the stage of injury. The positive effect of astrogliosis is to restrict the spread of inflammatory or toxic substances into normal neighboring tissue,[26] which may be helpful in the hyperacute phase to prevent further injury. The negative effect of astrogliosis is the effect of scarring, which could inhibit the ability of axonal regeneration in the chronic and recovery phases.[27] Potential drug treatments in TBI could target these cells to prevent the scarring seen in the chronic phase to allow axonal regeneration. MRI could offer a means to longitudinally target the optimal treatment time window in experimental TBI.

A similar ring and crescent-shaped enhancement of the MEMRI signal has been previously reported to correspond to the GFAP-positive astroglia observed in the peripheral region of the ischemic core 11 days after middle cerebral artery occlusion.[6] The investigators found good agreement between MEMRI signal enhancement and gliosis, predominantly GFAP-positive astrogliosis reacting to injury. In contrast, the presence of apoptotic cells and the size of the necrotic region (as evaluated by hematoxylin and eosin staining) did not agree with the area showing MEMRI signal enhancement. They suggested the increased Mn^{2+} accumulation in hyperactive microglia and the migration of reactive microglia around the injury contributed to the MEMRI enhancement in ischemic stroke.

Similarly, co-localization of enhanced MEMRI with the distribution of GFAP, Mn^{2+}-superoxide dismutase, and glutamine synthetase immunoreactivities has been reported in ischemic brain injury.[28] Mn^{2+} binds to the mitochondrial Mn^{2+}-superoxide

dismutase enzyme, which acts against cellular oxidative stress. It also binds to glutamine synthetase, a glial specific enzyme for regulating extracellular glutamate and reducing glutamate excitotoxicity. It has been suggested that an exogenous Mn^{2+} injection might provide enhanced MEMRI detection of oxidative stress and gliosis early after brain ischemia.

Comparison with lesion volume and behavioral scores

We found that lesion volume and behavioral score profiles herein are consistent with those reported previously using an identical model of TBI.[17,29] We previously reported that, in the S1FL, T2 increased and fractional anisotropy decreased at 3 h after TBI and gradually returned toward normal by day 14. The apparent diffusion coefficient increased at 3 h, peaked on day 2, and gradually returned toward normal at day 14. The peak of T2 lesion volume on day 2 was associated with vasogenic edema, consistent with behavioral score profiles. By contrast, the MEMRI contrast has a markedly different temporal profile with a signal void at the center of the lesion and enhancement surrounding the lesion that was most apparent on days 7 and 14. Correlation analysis revealed significant correlation between IR T1-weighted MEMRI intensity profiles and behavioral scores.

Potential pitfall and future directions

We used IR T1-weighted MRI because it yielded better contrast than T1 maps and higher temporal resolution. If quantitation is desired, T1 measurements can be made albeit with longer acquisition time but would not alter the overall conclusion. MEMRI may also be used to investigate T1-weighted signal enhancements with other histological markers for secondary injuries including: inflammation and oxidative stress, among others, with animals sacrificed at each time point. Future studies will use MEMRI to study chronic TBI, apply other MRI techniques, evaluate changes in functional connectivity using site-directed injection of Mn^{2+} in or around the cortex below the impact, target treatment time window, and monitor functional reorganization and recovery in TBI.

Conclusions

This study demonstrates the novel MEMRI application in experimental TBI. MEMRI detected early indications of excitotoxic injury and BBB disruption that preceded vasogenic edema in the hyperacute phase. In the subacute phase, MEMRI detected changes consistent with reactive gliosis. If indeed MEMRI is sensitive to gliosis and other biological processes, MEMRI can be used to target optimal treatment time window for TBI. MEMRI offers novel contrast that complements conventional MRI in the study of TBI.

Author Disclosure Statement

No competing financial interests exist.

References

1. Coronado, V.G., McGuire, L.C., Sarmiento, K., Bell, J., Lionbarger, M.R., Jones, C.D., Geller, A.I., Khoury, N., and Xu, L. (2012). Trends in traumatic brain injury in the U.S. and the public health response: 1995–2009. J. Safety Res. 43, 299–307.
2. Werner, C., and Engelhard, K. (2007). Pathophysiology of traumatic brain injury. Br. J. Anaesth. 99, 4–9.
3. Blennow, K., Hardy, J., and Zetterberg, H. (2012). The neuropathology and neurobiology of traumatic brain injury. Neuron 76, 886–899.
4. Young, W. (1992). Role of calcium in central nervous system injuries. J. Neurotrauma, Suppl 1, S9–S25.
5. Trump, B.F., and Berezesky, I.K. (1995). Calcium-mediated cell injury and cell death. FASEB J 9, 219–228.
6. Kawai, Y., Aoki, I., Umeda, M., Higuchi, T., Kershaw, J., Higuchi, M., Silva, A.C., and Tanaka, C. (2010). In vivo visualization of reactive gliosis using manganese-enhanced magnetic resonance imaging. Neuroimage 49, 3122–3131.
7. Du, S., Rubin, A., Klepper, S., Barrett, C., Kim, Y.C., Rhim, H.W., Lee, E.B., Park, C.W., Markelonis, G.J., and Oh, T.H. (1999). Calcium influx and activation of calpain I mediate acute reactive gliosis in injured spinal cord. Exp. Neurol. 157, 96–105.
8. Silva, A.C., Lee, J.H., Aoki, I. and Koretsky, A.P. (2004). Manganese-enhanced magnetic resonance imaging (MEMRI): methodological and practical considerations. NMR Biomed 17, 532–543.
9. Lin, Y.J., and Koretsky, A.P. (1997). Manganese ion enhances T1-weighted MRI during brain activation: an approach to direct imaging of brain function. Magn. Reson. Med. 38, 378–388.
10. Duong, T.Q., Silva, A.C., Lee, S.P., and Kim, S.G. (2000). Functional MRI of calcium-dependent synaptic activity: cross correlation with CBF and BOLD measurements. Magn. Reson. Med. 43, 383–392.
11. Pautler, R.G., and Koretsky, A.P. (2002). Tracing odor-induced activation in the olfactory bulbs of mice using manganese-enhanced magnetic resonance imaging. Neuroimage 16, 441–448.
12. Tucciarone, J., Chuang, K.H., Dodd, S.J., Silva, A., Pelled, G., and Koretsky, A.P. (2009). Layer specific tracing of corticocortical and thalamocortical connectivity in the rodent using manganese enhanced MRI. Neuroimage 44, 923–931.
13. van der Zijden, J.P., Wu, O., van der Toorn, A., Roeling, T.P., Bleys, R.L., and Dijkhuizen, R.M. (2007). Changes in neuronal connectivity after stroke in rats as studied by serial manganese-enhanced MRI. Neuroimage 34, 1650–1657.
14. Smith, K.D., Kallhoff, V., Zheng, H., and Pautler, R.G. (2007). In vivo axonal transport rates decrease in a mouse model of Alzheimer's disease. Neuroimage 35, 1401–1408.
15. Kivity, S., Tsarfaty, G., Agmon-Levin, N., Blank, M., Manor, D., Konen, E., Chapman, J., Reichlin, M., Wasson, C., Shoenfeld, Y., and Kushnir, T. (2010). Abnormal olfactory function demonstrated by manganese-enhanced MRI in mice with experimental neuropsychiatric lupus. Ann. N. Y. Acad. Sci. 1193, 70–77.
16. Bouilleret, V., Cardamone, L., Liu, Y.R., Fang, K., Myers, D.E., and O'Brien, T.J. (2009). Progressive brain changes on serial manganese-enhanced MRI following traumatic brain injury in the rat. J. Neurotrauma 26, 1999–2013.
17. Watts, L.T., Long, J.A., Chemello, J., Van Koughnet, S., Fernandez, A., Huang, S., Shen, Q., and Duong, T.Q. (2014). Methylene blue is neuroprotective against mild traumatic brain injury. J. Neurotrauma 31, 1063–1071.
18. Shen, Q., Meng, X., Fisher, M., Sotak, C.H., and Duong, T.Q. (2003). Pixel-by-pixel spatiotemporal progression of focal ischemia derived using quantitative perfusion and diffusion imaging. J. Cereb. Blood Flow Metab. 23, 1479–1488.
19. Shen, Q., Ren, H., Cheng, H., Fisher, M. and Duong, T.Q. (2005). Functional, perfusion and diffusion MRI of acute focal ischemic brain injury. J. Cereb. Blood Flow Metab. 25, 1265–1279.
20. Meng, X., Fisher, M., Shen, Q., Sotak, C.H., and Duong, T.Q. (2004). Characterizing the diffusion/perfusion mismatch in experimental focal cerebral ischemia. Ann. Neurol. 55, 207–212.
21. Obenaus, A., Robbins, M., Blanco, G., Galloway, N.R., Snissarenko, E., Gillard, E., Lee, S. and Curras-Collazo, M. (2007). Multi-modal magnetic resonance imaging alterations in two rat models of mild neurotrauma. J. Neurotrauma 24, 11471160.
22. Li, W., Long, J.A., Watts, L.T., Jiang, Z., Shen, Q., Li, Y., Duong, T.Q. (2014). A quantitative MRI method for imaging blood brain barrier leakage in experimental traumatic brain injury. Plos One 9, e114173.
23. De La Garza, B.H., Li, G., Shih, Y.Y., and Duong, T.Q. (2012). Layer-specific manganese-enhanced MRI of the retina in light and dark adaptation. Invest. Ophthalmol. Vis. Sci. 53, 4352–4358.
24. Chodobski, A., Zink, B.J., and Szmydynger-Chodobska, J. (2011). Blood-brain barrier pathophysiology in traumatic brain injury. Transl. Stroke Res. 2, 492–516.

25. Henning, E.C., Meng, X., Fisher, M., and Sotak, C.H. (2005). Visualization of cortical spreading depression using manganese-enhanced magnetic resonance imaging. Magn. Reson. Med. 53, 851–857.
26. Fitch, M.T., and Silver, J. (1997). Glial cell extracellular matrix: boundaries for axon growth in development and regeneration. Cell Tissue Res. 290, 379–384.
27. McGraw, J., Hiebert, G.W., and Steeves, J.D. (2001). Modulating astrogliosis after neurotrauma. J. Neurosci. Res. 63, 109–115.
28. Chan, K.C., Cai, K.X., Su, H.X., Hung, V.K., Cheung, M.M., Chiu, C.T., Guo, H., Jian, Y., Chung, S.K., Wu, W.T., and Wu, E.X. (2008). Early detection of neurodegeneration in brain ischemia by manganese-enhanced MRI. Proceedings of the Annual International Conference of the IEEE Engineering in Medicine and Biology Society. IEEE Engineering in Medicine and Biology Society. 2008, 3884–3887.
29. Long, J.A., Watts, L.T., Chemello, J., Huang, S., Shen, Q., and Duong, T.Q. (2014). Multiparametric and longitudinal MRI characterization of mild traumatic brain injury in rats. J. Neurotrauma. Epub ahead of print.

Address correspondence to:
Timothy Q. Duong, PhD
Research Imaging Institute
University of Texas Health Science Center at San Antonio
8403 Floyd Curl Drive
San Antonio, TX 78229

E-mail: duongt@uthscsa.edu